*Advanced Materials Research* *Online: 2014-08-11*
*ISSN: 1662-8985, Vol. 996, pp 634-639*
*doi:10.4028/www.scientific.net/AMR.996.634*


# Predicting the Effects of Grain Size on Machining-induced Residual Stresses in Steels

Mohamed N. A. Nasr

Dept. of Mechanical Engineering, Faculty of Engineering, Alexandria University, Alexandria, Egypt

Adjunct – Dept. of Materials Science & Engineering, Egypt-Japan University of Science & Technology, Alexandria, Egypt

M.Nasr@alexu.edu.eg

**Keywords:** Machining; Residual stresses; Grain size; Finite element modelling (FEM); Steels.

**Abstract.** The current study examines the effect of grain size on macro-scale machining-induced residual stresses (RS), during turning, using finite element modelling. Based on the well-established inverse relation between grain size and material strength, the grain size effect was simulated via changing the workpiece yield strength. This was also done at different strain hardening rates. The model was validated using four materials. Larger grain size (lower yield strength) resulted in higher surface tensile RS, which is attributed to the surface layer being subjected to higher compressive plastic deformation as well as higher workpiece temperatures.

## Introduction

Fine-grained steels typically have higher tensile strength according to the well-established Hall-Petch relation, which assumes an inverse square-root dependence of strength upon average grain size [1 - 4]. The grain size effect even extends to other mechanical properties, like hardness, wear resistance and fatigue life [1, 5]. In addition, grain refinement results in lower ductile-to-brittle transition temperature and increases the penetration depth of X-rays [1], which are used to measure residual stresses (RS).

The effect of grain size on mechanical properties is mainly attributed to grain-boundary strengthening, which is affected by four main factors as identified by Hu et al. [2]. These four factors are; 1) grain boundaries act as barriers to plastic flow; 2) grain boundaries act as dislocation sources; 3) elastic anisotropy, resulting from different grain orientation, causes additional stresses in grain-boundary surroundings; and 4) multi-slip is activated in the grain boundary regions, whereas grain interiors are initially dominated by single slip. The overall effect of the aforementioned parameters is the formation of work hardened layers along grain boundaries, which is more pronounced in fine-grained materials [2].

With regards to grain size effects, the main focus of the literature was on correlating grain size to material mechanical properties. Hu et al. [2] presented a constitutive model to predict plastic flow stress as function of grain size. At large grain sizes (order of microns), the Hall-Petch relation was found to be valid; however, in the nano-crystalline domain the material flow stress approached that of the grain boundaries. Berbenni et al. [4] presented a theoretical micromechanical model to examine the effect of grain size distribution on yield strength. The authors showed that the overall yield stress depends not only on the mean grain size but also on the grain size dispersion, especially for fine-grained materials. It is important to point out that, Dunstan and Bushby [6] presented an updated study (2014) on the applicability of the Hall-Petch relation, where they examined the applicability of other mathematical formulas (modifications of the Hall-Petch formula). The modified formulas succeeded in correlating the grain size to material strength; however, the degree of dependability differs from a material to another.

The effect of grain size on fatigue crack growth in pure titanium was examined by Tokaji et al. [5], under reversed axial loading and rotating bending. Small cracks were found to grow faster than large cracks, with higher growth rate in coarse-grained materials. This was attributed to the less significant effects of microstructure (grain boundaries and crack deflection) in coarse-grained materials.

Other studies have examined the role of grain size in machining processes. M'Saoubi and Chandrasekaran [7] studied the role of material phase and grain size on chip formation and work hardening, during orthogonal machining of single and dual phase steels. Results indicated a strong effect of material phase on primary chip parameters, work hardening and tool chip friction, but limited effect of grain size. In addition, grain size distribution was found to affect chip parameters, where a uniform distribution resulted in reduced scatter of chip parameters. The study covered grain sizes within the industrial range (45–130 μm). In a study by Gotoh et al. [1], the effect of grain size on RS after grinding of steels was examined. Two types of steels, having the same chemical composition, were used; a fine-grained rolling steel "NFG600" (average grain size of 3 μm) and a conventional rolling steel "SM490" (average grain size of 15μm). Results showed that NFG600 experienced compressive RS, while SM490 experienced tensile RS.

Wang et al. [8] examined the effect of annealing and grain orientation on RS when cold rolling stainless steel AISI 301. The authors used neutron diffraction to measure grain-orientation-dependent RS, or inter-granular RS. Annealing was found to reduce orientation anisotropy of RS, and consequently reduced inter-granular RS. Also, local RS were found to vary greatly within a grain based on its orientation. Micro-machining of AISI 1045 steel was studied by Simoneau et al. [9], where the authors focused on the effect of grain size and orientation on surface defects. This was done experimentally and numerically using finite element analysis (FEA). Grain refinement (~ 20 μm) was found to reduce surface dimples when compared to normal grain size (~ 100 μm), especially when grain boundaries are not oriented along the shear plane.

Residual stresses are typically categorized, on a length scale, into three categories. Type I stress, which varies on the scale of multiple grains; type II stress (inter-granular), which varies from grain to another; and, type III stress which fluctuates within a grain. Traditionally, type I stress is referred to as "macro-stress"; however, types II and III are referred to as "micro-stress". The current study is concerned with macro-scale RS (type I) resulting from machining processes, and how they are affected by average grain size. A special focus is given to RS in the cutting direction (RS11). Based on the Hall-Petch relation, the current work examines the effect of grain size in terms of material yield strength. A set of finite element (FE) models was built, using the commercial FE software ABAQUS, to simulate orthogonal dry cutting of steels and predict the resulting RS.

**Finite Element Modelling (FEM)**

Two plane strain two-dimensional FE models were built, using the commercial FE software ABAQUS, in order to simulate the effects of grain size on RS. Fig. 1 shows the first model that was used to simulate the process of orthogonal cutting using the arbitrary-Lagrangian-Eulerian (ALE) technique, available in ABAQUS/Explicit. The workpiece was divided into four regions (*A* – *D*); regions *A*, *C* and *D* were Lagrangian regions with adaptive remeshing, while region *B* was an Eulerion region. The cutting velocity was applied to the workpiece, while the tool was fixed. A detailed description of the cutting model as well as the advantages of using ALE in modelling the cutting process was previously published in [10]. The second model was used for RS (type I) prediction using a non-traditional time-efficient approach that was developed by the author in 2008 [11]. RS prediction was done using ABAQUS/Standard, with a special focus on RS11. Details of the time-efficient RS approach, as well as the reasons for using explicit solvers in modelling the cutting process could be found in [11]. Coupled temperature–displacement analysis was used in both models, in order to allow for temperature-dependent properties and heat transfer.

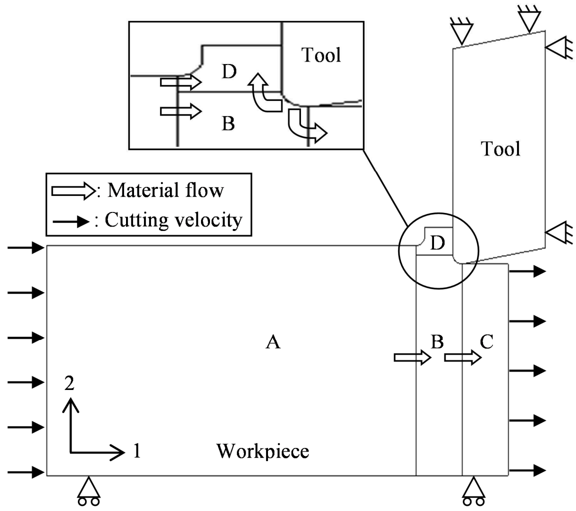


Fig. 1: ALE cutting model (hollow arrows show material flow between different regions)

**Model Validation.** The current FE model was validated by comparing the predicted RS11 profiles to experimental profiles obtained under similar cutting conditions, for four different materials. These materials are AISI 316L (165 HV) stainless steel, AISI 4340 (30 HRc) steel, AISI 52100 (62 HRc) hardened steel, and AISI H13 (52 HRc) tool steel. Detailed validation was published in [12], and Fig. 2 and Fig. 3 show the AISI 316L and AISI 4340, respectively, as an example.

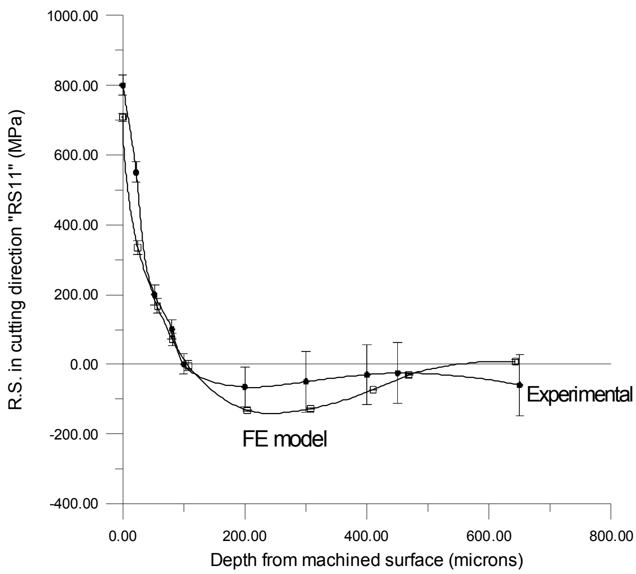


Fig. 2: Model validation AISI 316L stainless steel (experimental results were obtained from [13])

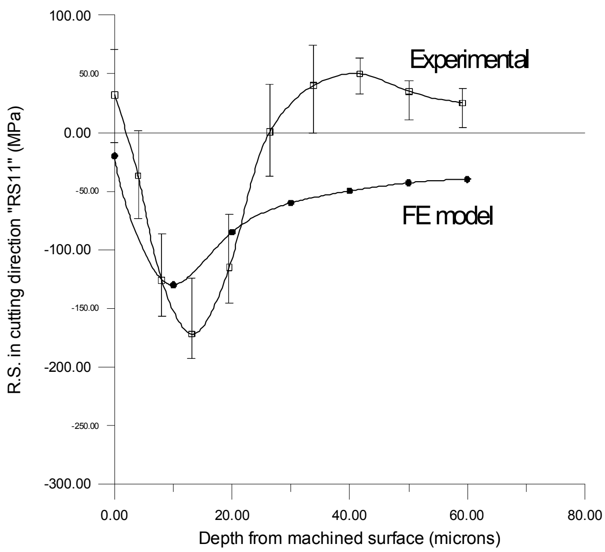


Fig. 3: Model validation AISI 4340 steel (experimental results were obtained from [14])

**Workpiece Material Properties.** The Johnson-Cook (J-C) constitutive model [15], given by Eq. 1, was used to describe the plastic behaviour of the workpiece material. Since this model takes the effects of temperature, strain rate, and strain hardening into account, it is suitable for modelling the metal cutting process [10, 11, 12]. The J-C parameters of the four materials used for model validation are given in Table 1.

$$\sigma = (A + B\varepsilon^n)\left(1 + C\ln\left(\frac{\dot{\varepsilon}}{\dot{\varepsilon_0}}\right)\right)\left(1 - \left(\frac{T - T_r}{T_m - T_r}\right)^m\right) \quad (1)$$

Where:

σ: Current von Mises flow stress
*A*: Initial yield strength
*B*: Strain hardening coefficient
*n*: Strain hardening exponent
*m*: Thermal softening exponent
*C*: Strain rate coefficient
ε: Equivalent plastic strain
$\dot{\varepsilon}$: Equivalent plastic strain rate
$\dot{\varepsilon}_0$: Reference plastic strain rate
*T:* Current temperature
$T_r$: Reference temperature
$T_m$: Melting temperature

Table 1: J-C parameters for AISI 316L, AISI H13, AISI 52100 and AISI 4340 [12]

| Material | *A* [MPa] | *B* [MPa] | *n* | *C* | $\dot{\varepsilon}_o$ [$s^{-1}$] | *m* |
|---|---|---|---|---|---|---|
| AISI 316L | 305 | 1161 | 0.61 | 0.01 | 1 | 0.517 |
| AISI H13 | 715 | 329 | 0.28 | 0.03 | 3500 | 1.5 |
| AISI 52100 | 774 | 134 | 0.37 | 0.017 | 1 | 3.17 |
| AISI 4340 | 792 | 510 | 0.26 | 0.014 | 1 | 1.03 |

In order to numerically predict the effects of grain size on RS (type I), it was essential to identify the J-C constitutive model parameters (or another suitable numerical constitutive model); however, no data was available in the literature. Accordingly, the current work depended on the inverse relation between the average grain size and material strength (Hall-Petch relation). This was done via running simulations with materials having different yield strengths (*A* in Eq. 1). Three qualitative levels of grain sizes were assumed; fine "F", medium "M" and coarse "C". The corresponding *A* values selected in the current study, to numerically represent the aforementioned grain sizes, are 900 MPa, 600 MPa and 300 MPa, respectively. This was based on the literature in order to cover a wide variety of commercial steels. In addition, different strain hardening rates (*B* & *n* parameters in Eq. 1) were used. The full test matrix, shown in Table 2, covers a wide range of steels taking into consideration the interaction between yield, strain hardening and grain size. All other material properties were kept constant and similar to those of AISI 316L, for model validation purposes.

Table 2: Test matrix with different *A*, *B* & *n* values

| *A* [MPa] | 300 (≡ coarse size "C") | | | 600 (≡ medium size "M") | | | 900 (≡ fine size "F") | | |
|---|---|---|---|---|---|---|---|---|---|
| *B* [MPa] | 300 | 600 | 900 | 300 | 600 | 900 | 300 | 600 | 900 |
| *n* | 0.3 & 0.6 | | | | | | | | |

**Cutting Conditions.** For model validation purposes, cutting conditions were selected similar to those in [12]. An uncoated carbide (Kennametal K313) cutting insert with zero rake angle along with cutting speed of 125 m/min and uncut chip thickness of 0.1 mm were used. The insert was assumed to be sharp with edge radius of 20 μm. Tool physical properties were obtained from [12].

**Friction and Heat Generation / Dissipation.** The simple Coulomb friction model, which assumes constant coefficient of friction along the tool–workpiece contact length, was used in the current work. Although it is a simple unrealistic model, it has been widely used in metal cutting simulations [10, 11, 12] because the real coefficient of friction cannot be measured any ways; besides, it gives reasonable results. A coefficient of friction of 0.2 was assumed in the current work. Ninety per cent (90%) of the plastic deformation mechanical energy was assumed to be converted into heat. This is based on data available in the literature [10, 11, 12]. Heat radiation and convection were neglected in the cutting model, as they are negligible compared to conduction. In the stress relaxation model, convection to air was considered with a coefficient of heat convection of 10 $W/m^{2o}C$ and sink temperature of 20 $^oC$.

## Results and Discussion

Fig. 4a and Fig. 4b show the effect of yield strength (*A*) on surface RS11 for different *B* values at *n* = 0.3 & 0.6, respectively. In the figures, the grain size is represented by either "C" for "coarse", "M" for "medium" or "F" for "fine". Materials with finer grains (higher yield strength "*A*") experienced lower surface tensile RS11, at all strain hardening rates (*B* & *n* values). This effect is more evident at higher hardening rates. In other words, grain refinement would result in lower tendency for surface tensile RS11 (or higher surface compressive RS11). It is worth mentioning that, the current results are in agreement with the experimental results of Gotoh et al. [1], when they grinded two types of steel; a fine-grained rolling steel "NFG600" and a conventional rolling steel "SM490".

A coarse-grained material would be easier to deform compared to a fine-grained material, when subjected to the same loading conditions, because the former has lower yield strength. Therefore, a coarse-grained material would experience higher plastic deformation, as predicted by the current results shown in Table 3, where materials with lower *A* values experienced more compressive plastic strains in the cutting direction "PE11". Since compressive (negative) plastic deformation results in tensile RS [16, 17], this explains the aforementioned results. In addition, higher temperatures were generated in coarse-grained materials (lower *A* values), as shown in Table 4, which also adds to the generation of surface tensile RS [17, 18]. Such increase in workpiece temperature is attributed to heat generation resulting from plastic deformation.

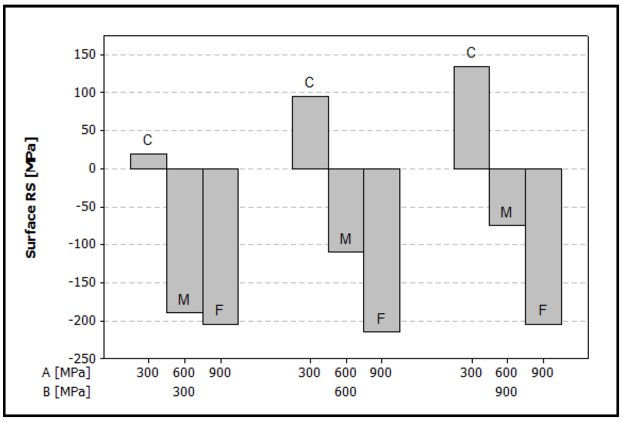


a) *n* = 0.3

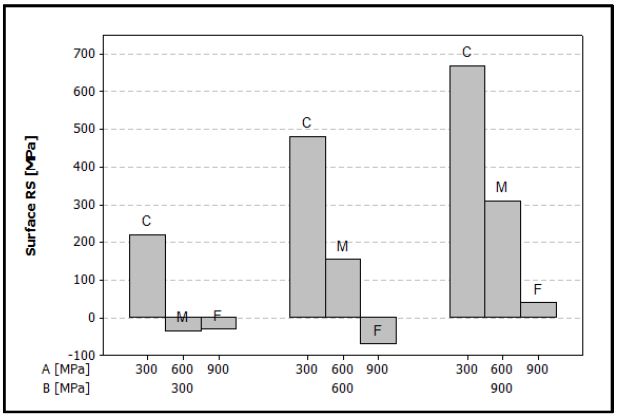


b) *n* = 0.6

Fig. 4: Effect of grain size (yield "*A*") on surface RS11
(Grain size coding: C ≡ coarse, M ≡ medium & F ≡ fine)

Table 3: Effect of grain size (yield "*A*") on plastic strain in cutting direction "PE11"
(B = 900 MPa)

| *n* | 0.3 | | | 0.6 | | |
|---|---|---|---|---|---|---|
| *A* [MPa] | 300 "C" | 600 "M" | 900 "F" | 300 "C" | 600 "M" | 900 "F" |
| PE11 | -0.345 | 0.330 | 0.325 | -0.380 | -0.345 | -0.330 |

Table 4: Effect of grain size (yield "*A*") on workpiece temperature underneath tool
(B = 900 MPa)

| *n* | 0.3 | | | 0.6 | | |
|---|---|---|---|---|---|---|
| *A* [MPa] | 300 "C" | 600 "M" | 900 "F" | 300 "C" | 600 "M" | 900 "F" |
| Temperature [$^{o}$C] | 328 | 330 | 300 | 510 | 440 | 425 |

## Summary

The effect of grain size on RS (type I) was investigated using FEM. Three levels of grain sizes were assumed; fine, medium and coarse. Based on the inverse relation between grain size and material strength (Hall-Petch relation), fine grains correspond to higher yield strength. Accordingly, the effect of grain size on RS was simulated by assigning three different values for yield strength; 900 MPa, 600 MPa and 300 MPa, respectively. This was also done at different strain hardening rates. Larger grain size (lower yield strength) resulted in higher surface tensile RS, which was attributed to higher compressive plastic deformation and higher workpiece temperatures. The current results also agree with the experimental findings of Gotoh et al. [1].


## References


[1] M. Gotoh, K. Seki, M. Shozu, H. Hirose, and T. Sasaki, Influence of steel grain size on residual stress in grinding processing, Mater. Sci. Forum 638-642 (2010) 2389-94.

[2] H.-H. Fu, D.J. Benson, and M. A. Meyers, Analytical and Computational Description of effect of grain size on yield stress of metals, Acta Mater. 49 (2001) 2567–82.

[3] C. Wei, S. Lin, R.G. Qian, and J.M. Hsiao, Computer simulation of effect of grain size on the properties of polycrystalline specimens by finite element method, Acta Mater. 39 (1991) 2051-57.

[4] S. Berbenni, V. Favier, and M. Berveiller, Impact of the grain size distribution on the yield stress of heterogeneous materials, Int. J. Plast. 23 (2007) 114–142.

[5] K. Tokaji, T. Ogawa, and K. Ohya, The effect of grain size on small fatigue crack growth in pure titanium, Int. J. Fatigue 16 (1994) 571-78.

[6] D.J. Dunstan and A.J. Bushby, Grain size dependence of the strength of metals: The Hall–Petch effect does not scale as the inverse square root of grain size, Int. J. Plast. 53 (2014) 56-65.

[7] R. M'Saoubi and H. Chandrasekaran, Role of phase and grain size on chip formation and material work hardening during machining of single and dual phase steels, Ironmaking Steelmaking 31 (2004) 258-264.

[8] Y.D. Wang, R. Lin Peng, X.L. Wang, and R.L. McGreevy, Grain-orientation-dependent residual stress and the effect of annealing in cold-rolled stainless steel, Acta Mater. 50 (2002) 1717-34.

[9] A.Simoneau, E. Ng, and M.A. Elbestawi, Grain size and orientation effects when microcutting AISI 1045 steel, Ann. CIRP 56 (2007) 57-60.

[10] M.N.A. Nasr, E-G. Ng, and M.A. Elbestawi, Modelling the effects of tool-edge radius on residual stresses when orthogonal cutting AISI 316L, Int. J. Mach. Tool Manu. 47 (2007) 401–411.

[11] M.N.A. Nasr, E-G. Ng, and M.A. Elbestawi, A modified time-efficient FE approach for predicting machining-induced residual stresses, Finite Elem. Anal. Des. 44 (2008) 149-161.

[12] M.N.A. Nasr, E-G. Ng, and M.A. Elbestawi, Effects of workpiece thermal properties on machining-induced residual stresses – thermal softening and conductivity, Proc. Inst. Mech. Eng., B J. Eng. Manuf. 221 (2007) 1387-1400.

[13] R. M'Saoubi, J.C. Outeiro, B. Changeux, J.L. Lebrun, and A.M. Dias, Residual Stress Analysis in Orthogonal Machining of Standard and Resulfurized AISI 316L Steels, J. of Mats Proc Tech, 96 (1999) 225-233.

[14] A.B. Sadat, Effect of High Cutting Speed on Surface Integrity of AISI 4340 Steel During Turning, Mats Sc Tech, 6-4 (1990) 371-375.

[15] G.R. Johnson and W.H. Cook, A constitutive model and data for metals subjected to large strains, high strain rates and high temperatures, Seventh Int. Symposium on Ballistics, Hague, Netherlands, April 1983, 541-547.

[16] C. Wiesner, Residual stresses after orthogonal machining of AISI 304: numerical calculation of thermal component and experiment results, Metall. Mater. Trans. A, 23 (1992) 989-996.

[17] C.R. Liu, A.C. Lin, and M.M. Barash, Thermal and mechanical stresses in the workpiece during machining, Prod. Eng. Div. (PED), 12 (1984) 181-191.

[18] C.R. Liu and M.M. Barash, The mechanical state of the sub-layer of a surface generated by chip-removal process - Part 2: cutting with a tool with flank wear, J. Eng. Ind. (1976) 1202-08.